

Study of the ability of self-assembled *N*-vinylcarbazole monolayers to protect copper against corrosion

CHUN-TAO WANG,¹ SHEN-HAO CHEN,^{*1,2} HOU-YI MA,¹ LAN HUA¹ and NAI-XING WANG¹

¹Department of Chemistry, Shandong University, Jinan 250100, P. R. China and

²State Key Laboratory for Corrosion and Protection, Shenyang 110015, P. R. China

(Received 17 January, revised 28 June 2002)

Abstract: *N*-Vinylcarbazole (NVC) monolayers were self-assembled on copper surfaces. The electrochemical properties of the copper surfaces modified by NVC self-assembled monolayers (SAMs) were investigated using polarization and electrochemical impedance spectroscopic (EIS) methods. The polarization measurements indicated that the NVC SAMs could reduce the rates of the anodic and cathodic reaction on the surface of copper electrodes in 0.5 mol dm⁻³ NaCl solution. The EIS results showed the NVC formed a closely packed film that was able to inhibit copper corrosion. X-Ray photoelectron spectroscopy (XPS) analysis of the copper samples and atomic adsorption analysis of the solution showed that the copper surfaces were covered by NVC SAMs, and the adsorption of NVC on the copper surfaces was accompanied with dissolution of Cu into the solution.

Keywords: self-assembled monolayers, *N*-vinylcarbazole, copper, EIS, XPS.

INTRODUCTION

Copper is an important metal in industrial applications, particularly, in microelectronics, but it can be easily oxidized in air, and chloride ions significantly promote the corrosion process in aqueous solution, such as seawater. Self-assembled monolayers are dense and ordered monolayers.^{1–3} In recent years, the technique has offered a convenient method to protect the metal from corrosion. There have been some reports on the application of self-assembled films to the protection of metals against corrosion.^{4–8} Laibinis and Whitesides reported that alkanethiols adsorbed from solution onto copper surfaces formed densely packed self-assembled monolayers (SAMs),⁴ which were found to be effective inhibitors of copper corrosion in air. Because of a high blocking effect, densely packed monolayers could be used as protective films for copper surfaces against corrosion. Feng *et al.* reported the corrosion protection of self-assembled alkanethiol monolayer on copper in a 0.51 mol dm⁻³ NaCl solution.⁵ Aramaki reported that the maximum protection efficiency to copper corrosion in 0.5 mol dm⁻³ NaSO₄.⁶ was 80.3 % for octadecanethiol

* Author to whom correspondence should be addressed. E-mail: shchen@edu.cn.

SAMs. In addition, Quan *et al.* studied the self-assembled monolayers of Schiff Bases on copper surfaces, which were formed through the combination of copper and N atoms in the Schiff Bases molecules.^{7,8} Castro *et al.* reported the growth of 2-mercaptobenzoxazole on Cu (100) surfaces.⁹

In this paper, *N*-vinylcarbazole (NVC) SAMs were prepared on copper surfaces, and their protective effect on copper corrosion was studied in NaCl solution using polarization and electrochemistry impedance spectroscopic (EIS) techniques. In order to understand the process of self-assembly and chemical interaction between the NVC and the substrate, X-ray photoelectron spectroscopy (XPS) and atomic absorption analysis were carried out.

EXPERIMENTAL

N-Vinylcarbazole (purity $\geq 99\%$ from Fluka) was dissolved in absolute ethanol to a concentration of 1 mmol dm^{-3} . Copper substrates ($17 \times 8 \text{ mm}$) were used for the X-ray photoelectron spectroscopy (XPS) measurements. The copper electrodes were made from, 99.9% copper rods of 5.8 mm diameter. The electrodes were embedded in epoxy resin and the exposed surface was polished with 400[#] and 2000[#] emery paper prior to each experiment.

The self-assembled monolayers were formed as follows: The electrode was polished, washed with tri-distilled water, and then was etched in a $6 \text{ mol dm}^{-3} \text{ HNO}_3$ solution for 15 s, rinsed with triply-distilled water and absolute ethanol as quickly as possible; and then immediately immersed in adsorbate solutions for various immersion times whereby self-assembled monolayers formed. After the formation of the SAMs, the electrode was rinsed with absolute ethanol, and triply-distilled water.

The electrochemical measurements were performed in a three-electrode cell. The reference electrode was a saturated calomel electrode (SCE) and the counter electrodes was a platinum sheet. All potentials in this paper are referred to the SCE.

Potentiostatic polarization and EIS measurements were performed with an IM6 electrochemical workstation (ZAHNER, Germany). The polarization curves were recorded within the potential region from -0.4 to 0.1 V at a scan rate of 1 mV/s . For the EIS measurements, a sinusoidal potential perturbation of 5 mV in amplitude was used with frequencies ranging from 60 kHz to 0.02 Hz . The EIS measurements of the SAMs covered copper electrodes were carried out in $0.5 \text{ mol dm}^{-3} \text{ NaCl}$ aqueous solutions at the corrosion potential after 30 min immersion at $20 \pm 2 \text{ }^\circ\text{C}$.

The XPS spectra of the NVC SAMs were taken using a PHI 5300 ESCA System (Perkin-Elmer, USA). The excitation source was $\text{MgK}\alpha$ radiation (photoelectron energy = 1253.6 eV). Take-off angles of 20° , 45° , 70° from the surface were employed. All the XPS analyses were performed at a pressure below $1 \times 10^{-6} \text{ Pa}$. Atomic absorption analysis was performed using an atomic absorption spectrophotometer 3510 (Agilent Technologies). The solutions were introduced into the flame by conventional aspiration and the absorbance was measured using an analytical wavelength of 324.9 nm . The lamp current and slit width were set at 2.0 mA and 0.5 nm , respectively.

RESULTS AND DISCUSSION

Polarization measurements

To investigate the influence of the immersion time on corrosion protection ability, self-assembled NVC monolayers were prepared on copper electrodes for different immersion times in NVC solutions. Their polarization curves were then measured after 30 min immersion in $0.5 \text{ mol dm}^{-3} \text{ NaCl}$ solutions. The polarization experiment for bare copper was performed under the same condition. Figure 1 shows the polarization curve for the bare copper electrode measured in a $0.5 \text{ mol dm}^{-3} \text{ NaCl}$ solution, together with the polar-

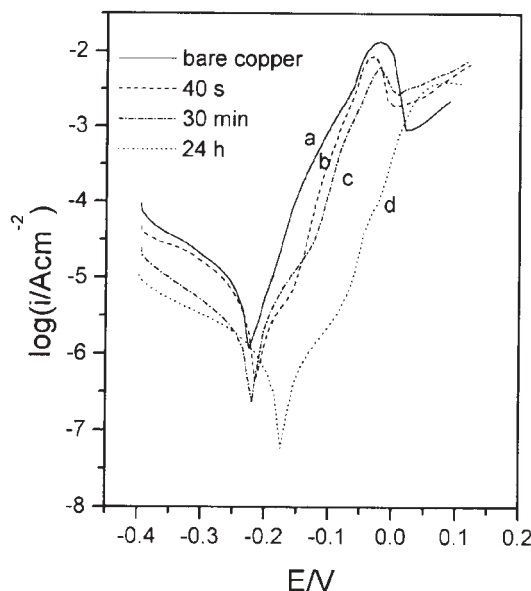


Fig. 1. Polarization curves for copper electrodes with and without NVC SAMs measured in a 0.5 mol dm^{-3} NaCl solutions at a sweep rate of 1 mV/s : (a) bare copper, (b) covered NVC SAMs with immersion time 40 s, (c) 30 min, (d) 24 h.

ization curves for copper electrodes covered with SAMs of NVC formed for different immersion times, 40 s, 30 min, 24 h. Compared with the polarization result of the bare electrode, as shown in Fig. 1a, lower anodic and cathodic current densities were observed in Fig. 1b, c and d. These results indicated that NVC SAMs could inhibit anodic and cathodic reactions. In general, the inhibition effect of the SAMs on copper corrosion increased gradually with increasing time of immersion. The polarization curve d, for 24 h immersion, showed the lowest anodic and cathodic current densities at the same potential.

The corrosion current densities (i_{corr}) were determined from the polarization curves by the Tafel extrapolation method. The inhibition efficiency ($P\%$) was calculated using the following formula:

$$P\% = \frac{i^0 - i}{i^0} \times 100\%$$

where i^0 and i are the corrosion current densities of bare copper electrode and SAMs covered electrode, respectively. The calculated results derived from Fig. 1 are listed in Table I. It was found that the inhibition efficiency was 70.2%, when the immersion time was 40 s. After 24 h immersion, the $P\%$ value rose to 93.8%.

It is known that the corrosion processes of copper in aerated NaCl solution comprise the anodic dissolution of copper and cathodic reduction of oxygen.^{10,11} The anodic dissolution of copper are shown in the following equations:



And the cathodic reduction of oxygen is as follows:



The NVC SAMs increased the charge-transfer resistance of the anodic dissolution of copper. Also, the NVC SAMs formed on the copper surface acted as a barrier the diffusion of oxygen molecules from the solution to the copper electrode. In addition, the corrosion potential of the copper electrode shifted positively after coverage by a NVC film during 24 h immersion, indicating that the NVC SAMs have a greater inhibition action on the anodic reaction than on the cathodic reaction.

TABLE I. The corrosion current densities obtained from Fig. 1 and the corresponding inhibition efficiencies

Immersion time	Corrosion current density/ $(\mu\text{A cm}^{-2})$	$P/\%$
0 (Bare copper)	7.65	
40 s	2.28	70.2
30 min	0.85	88.9
24 h	0.47	93.8

Electrochemistry impedance spectroscopy (EIS)

EIS has been used to characterize self-assembled monolayers by some authors.⁴⁻⁶ Some valuable electrochemical parameters, such as the coverage of the substrate by SAMs and the capacitance of the SAMs, could be obtained by means of EIS measurements. The Nyquist plots for a bare copper electrode in 0.5 mol dm^{-3} NaCl solution is presented in Fig. 2. It is known that the high-frequency capacitive loop can be attributed to the time constant of the charge-transfer resistance (R_t) and the double-layer capacitance (C_{dl}).^{12,13} The low-frequency linear portion is believed to be diffusion of soluble copper species (CuCl_2^-) from the electrode surface into the bulk solution.^{12,13} In addition to the experiment with a bare copper, a series of EIS experiments for copper electrodes covered with NVC SAMs formed after different immersion times in NVC ethanol solutions from 2 s to 26 h were performed.

In the high frequency region, the electrode reaction was controlled by a charge transfer process, and the diameter of the semicircle represents the charge transfer resistance (R_t).

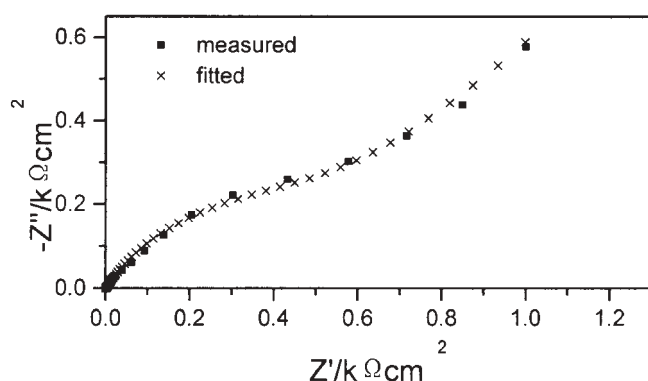
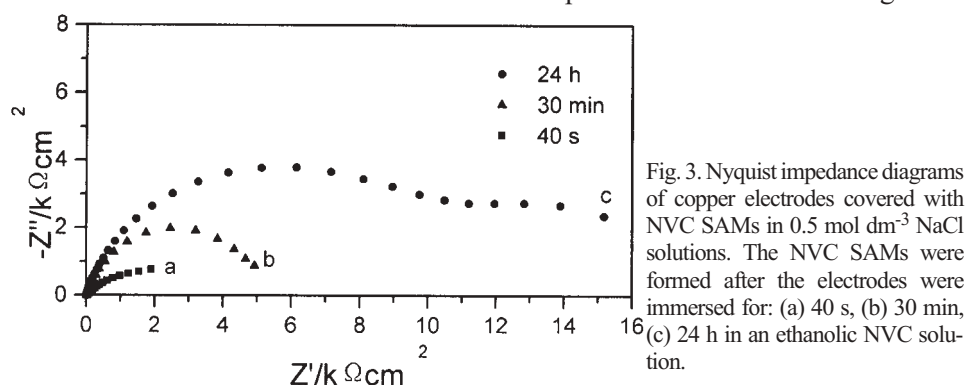


Fig. 2. Nyquist impedance diagram for a copper electrode measured in a 0.5 mol dm^{-3} NaCl solution.

Compared with the bare electrode, the NVC SAMs covered electrodes displayed a large capacitive loop in the high frequency region. Moreover, with increasing immersion time, Rt increased gradually (a, b, c in Fig. 3), showing that the coverage of the copper surface by SAMs increased steadily with immersion time in the NVC solutions. Besides, another capacitive loop was observed in curve c after 24 h immersion, which may be due to the different effect of the NVC SAMs on the anodic and cathodic reactions. The different effect of the NVC SAMs on the anodic and cathodic reactions was observed in the polarization curve shown in Fig. 1d.



If the electrochemical reaction is under diffusion control, the diffusion effect can be reflected in the low frequency region of the corresponding impedance diagram. For the bare copper electrode, as shown in Fig. 2, the Nyquist plot exhibits a Warburg impedance, indicating that mass transfer greatly affects the corrosion reactions. For the SAMs-covered copper electrodes (a, b, c in Fig. 3), the Warburg impedance disappeared at low frequencies, indicating the SAMs were sufficiently densely packed to prevent the copper substrates from corrosion in NaCl solution.¹⁴

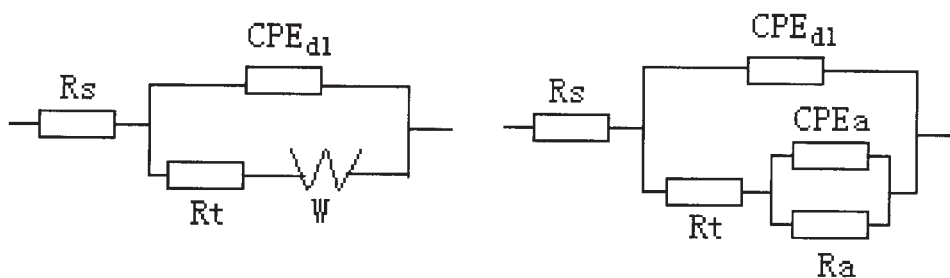


Fig. 4. Equivalent circuits used for fitting the impedance data in Figs. 2 and 3.

The equivalent circuits shown in Fig. 4 (a) and (b) were proposed to analyze the impedance plots for the bare and SAMs covered copper electrodes. Because the impedance plot in Fig. 2 reveals the effect of diffusion of soluble species, an equivalent circuit containing a Warburg impedance element was used (see Fig. 4a). In the equivalent circuits, W stands for the Warburg impedance, Rt the charge-transfer resistance, Rs the solution resis-

tance, R_a the pseudo-resistance. To obtain a good fit of the impedance data, the capacitors were substituted by constant phase elements (CPE). The impedance of a CPE is given by

$$Z_{\text{CPE}} = \frac{1}{Y_0} (j\omega)^{-n}$$

where Y_0 is the magnitude of CPE and n an empirical exponent ($n: 0 \leq n \leq 1$). The values of this empirical exponent indicate the distribution of time constants caused by inhomogeneities in the film.¹⁶ If $n = 1$, the impedance of a CPE is identical to the impedance of an ideal pure capacitor, and the impedance plot exhibits a perfect regular semicircle. The impedance plots in these experiments were represented by somewhat depressed semicircles due to the dispersing effect.¹⁷ It can be seen from Fig. 2 that the measured and fitted Nyquist plots of the bare copper correspond with each other. The measured and fitted Bode plots of the NVC SAMs covered electrodes, as in Fig. 3, are shown in Fig. 5, from which it can be seen that the fitted results coincide well with the measured results.

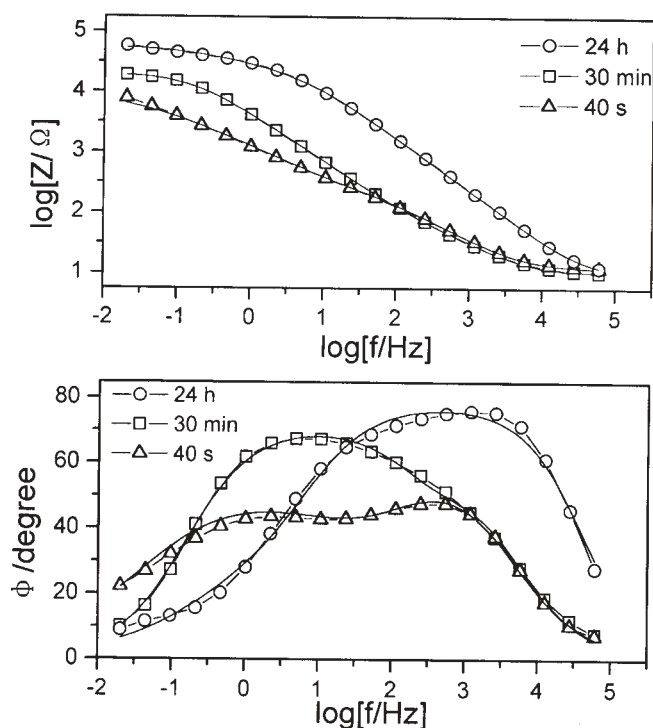


Fig. 5. Bode impedance diagrams of the measured and fitted impedance data in Fig. 2 and Fig. 3. The solid lines are fitted results.

The electrode coverage (θ) is the key factor that can be used to estimate the surface state of an electrode, and the charge transfer resistance is also related to it. Assuming that the corrosion reaction occurs at defect sites within the SAMs, the coverage of an electrode by SAMs can be calculated by^{14,15}

$$(1 - \theta) = \frac{Rt^0}{Rt}$$

where Rt^0 refers to the charge transfer resistance at bare copper and Rt the charge transfer resistance at the SAMs covered electrode measured under the same conditions. The main parameters of the fits of the impedance plots in shown in Figs. 2 and 3, and the values of coverage are listed in Table II. It can be seen that the values of the coverage given in Table II are slightly larger than the values of the inhibition efficiencies calculated from the polarization curves and shown in Table I. In general, the coverage increases with increasing immersion time. After 24 h immersion, the coverage reached a value of 94.8 %. The dependence of the surface coverage by NVC SAMs on the immersion time from 2 s to 26 h is shown in Fig. 6. At the beginning of self-assembly, the coverage increases markedly with increasing immersion time, then tends to a constant value of about 0.94. This result indicates that the formation process of the self-assembled SAMs can be classified by two typical steps, a fast adsorption in the early stages of the self-assembly, followed by rearrangement at a relatively slow rate.¹⁸ With increasing immersion time, the film becomes more compact and ordered. Therefore, to obtain a stable and densely self-assembled SAMs, the best immersion time is greater than 20 h. We consider that the saturated adsorption time is about 24 h, which is identical with the experimental result of Quan *et al.*⁷

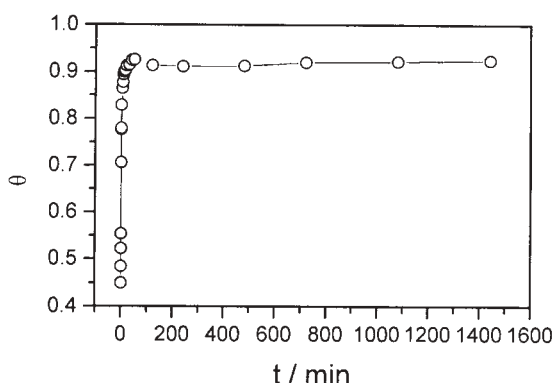


Fig. 6. Time dependence of the surface coverage for NVC SAMs on copper by immersing copper electrode in 1 mmol dm^{-3} NVC solutions.

The capacitance values of SAMs are usually used to characterize the quality of a self-assembled film. For a bare metallic electrode, the kinetic process is related to the charging-discharging process of the double layer capacitance. The capacitance charge across the film can be approximated from EIS,¹⁵ *i.e.*, assuming a parallel combination of a two parallel-plate capacitor, the first is assigned to the double-layer capacitance at the defects, and the second is assigned to the build up of charge across the film. The EIS can be used to evaluate the total capacitance (C_{total})¹⁵

$$C_{\text{total}} = C_{\text{dl}} + C_{\text{film}} = C_{\text{dl}}^0 (1 - \theta) + C_{\text{film}}^0 \theta$$

where C_{dl} is the capacitance at the defects, C_{film} is the capacitance across the film itself, C_{dl}^0 is the capacitance of pure copper and C_{film}^0 is the capacitance of a complete NVC

SAMs with 100 % coverage of the electrode surface. The values of C_{dl}^0 can be evaluated from the EIS spectrum of bare copper, and C_{total} can be evaluated from the EIS spectrum of the NVC SAMs covered copper. With θ measured independently, the defect-free film capacitance (C_{film}^0) can be calculated. Table III lists the calculated results derived from the coverage and capacitance values in Table II.

TABLE II. Element values of the equivalent circuits in Fig. 4, required for fitting the impedance spectra in Figs. 2 and 3

Immersion time	$Rt(k\Omega\text{ cm}^2)$	CPE_{dl}		$\theta/\%$
		$C/\mu\text{F cm}^{-2}$	n	
0 (Bare copper)	0.549	23.8	0.548	
40 s	2.67	20.1	0.751	79.4
30 min	6.98	15.8	0.797	92.1
24 h	10.6	2.61	0.871	94.8

It was found that both C_{total} and C_{film}^0 of each film covered copper electrode were smaller in comparison to the bare copper, since the dielectric constant of the adsorbed NVC is lower than water. For 24 h immersion in an ethanolic NVC solution, the values of C_{total} and C_{film}^0 were reduced to $2.61\ \mu\text{F cm}^{-2}$ and $1.33\ \mu\text{F cm}^{-2}$, respectively. So it can be inferred that the packing density of a film increases with increasing immersion time.

TABLE III. Capacitance of the NVC SAMs on copper derived from the EIS results of Table II

Immersion time	$\theta/\%$	$C_{total}/\mu\text{F cm}^{-2}$	$C_{film}^0/\mu\text{F cm}^{-2}$
0 (Bare copper)		23.8	
40 s	79.4	20.1	19.1
30 min	92.1	15.8	15.0
24 h	94.8	2.61	1.33

XPS Analysis

XPS Spectra of the NVC SAMs covered copper were performed to obtain composition information of the adsorption. Using a 45° take-off angle, the elements Cu, C, N, O were detected. After a copper substrate had been immersed in a $1\ \text{mmol dm}^{-3}$ NVC solution for 24 h the surface atomic composition was Cu 3.30, C 65.62, N 2.57 and O 28.51. The XPS spectra of Cu2p and N1s for NVC SAMs-covered copper and the CuLMM Auger spectra of copper covered with NVC SAMs, after the copper substrate had been in a $1\ \text{mmol dm}^{-3}$ NVC solution for 24 h. The Cu2p_{3/2} peaks at a binding energy (BE) of 932.4 eV and the Cu2p_{1/2} peaks at 952.4 eV can be attributed to either Cu(0) or Cu(I), which is hardly distinguishable in the Cu2p spectra by the 0.1 eV BE shift. Cu(II) which is located at a BE of 933.5 eV,⁵ was not found in the spectra. The Cu LMM Auger spectra of copper covered with NVC SAMs shows the existence of both Cu(0) and Cu(I), which are located at 335.0 and 337.0 eV, respectively. The relatively high peak of Cu(0) may be caused by

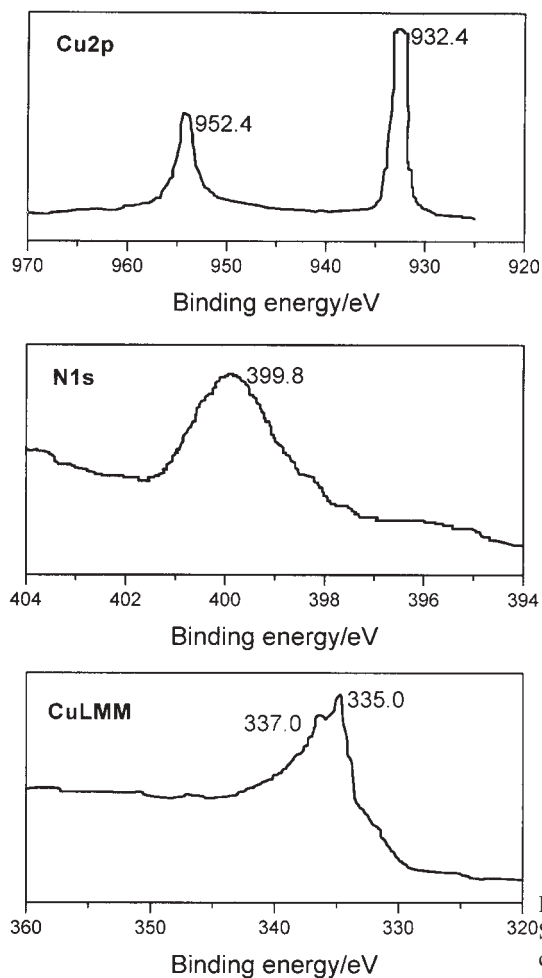


Fig. 7. XPS spectra of Cu2p and N1s for NVC SAMs on Cu and Cu LMM Auger spectra of copper covered with NVC SAMs

the copper substrate, while Cu(I) existed in the NVC self-assembled SAMs. The N1s peak at 399.8 eV indicated the adsorption of the NVC. Also, the existence of oxygen in the SAMs showed that the oxygen dissolved in the solution had taken part in the self-assembly process, either oxidizing some of the Cu atoms on the substrate surface or promoting the NVC adsorption on the copper surface, which is similar to the adsorption of thiols on an Au surface.¹⁹

TABLE IV. Atomic percentage for NVC SAMs covered copper obtained by XPS analysis with different take-off angles

Take off angles	Cu	C	O	N
20°	4.70	67.56	25.92	1.81
45°	3.30	65.62	28.51	2.57
70°	2.96	64.33	30.05	2.67

To determine the interaction between the copper surface and NVC molecules, the atomic percentage of the NVC SAMs covered copper was measured using different take-off angles, 20, 45, and 70°. The results are listed in Table IV. It can be seen that the atomic percentage of N increases with increasing take off angle, which suggests that the NVC molecules are adsorbed to the copper surface through the N atoms. The self-assembled process occurs *via* a complexing reaction of Cu(I) and NVC molecules.

Atomic absorption analysis

After the adsorption process, the residual solution was subjected to atomic absorption analysis. A stock standard Cu solution (1 mg ml⁻¹) was prepared. Working standard solutions were obtained by diluting the stock standard solution to 0.400, 0.800, 1.200, 1.600 mg l⁻¹. Then the absorbance of the solutions was measured to obtain a calibration graph. The obtained calibration graph shown in Fig. 8 is linear over the range of 0.30 – 1.70 mg l⁻¹ when the Beer law is obeyed. The linear-regression equation is as follows:

$$A = 0.004000 + 0.164000/c \quad (4)$$

where A is the absorbance and c the concentration of the solutions. The linear correlation coefficient R was 0.9966. From the calibration graph, the residual solution was found to contain 2.5 µg ml⁻¹ copper. This result suggests that during the self-assembly process, dissolution of copper into the solution occurs.

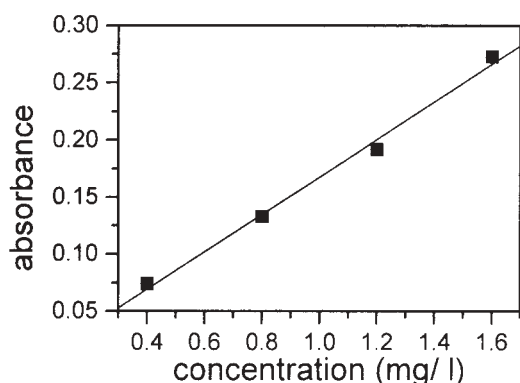


Fig. 8 Calibration graph for stock standard Cu solutions obtained by atomic absorption analysis.

The existence of oxygen in the adsorbate solution may be the key reason for the copper dissolution. As the adsorption of NVC on the copper surface progresses, as the oxygen in the adsorbate solution acts as an oxidant and then the dissolution of the copper occurs. In the early stages of the self-assembly progress, the adsorption of NVC and the dissolution of Cu occur simultaneously. As the number of NVC molecules adsorbed on the copper surface increases, the subsequent dissolution of Cu can be inhibited.

CONCLUSIONS

NVC can be rapidly self-assembled onto a copper surface. The maximum attainable coverage is 94.8 %. The NVC self-assembled SAMs efficiently inhibit corrosion of the

copper in NaCl solution by inhibiting the dissolution of copper and retarding the reduction of dissolved oxygen. The inhibition efficiency can reach 93.8 %. The formation process of the self-assembled SAMs can be classified by two typical steps, fast adsorption in the initial state, followed by rearrangement at a relatively slow rate. The longer the time the copper is immersed in the NVC solution, the higher is the quality of the film formed on the copper surface. XPS demonstrated that the NVC molecules are linked to the copper surface by N atom and that complexation of Cu(I) and NVC may occur. During the self-assembly process, copper dissolution into the solution occurred simultaneously.

Acknowledgements: This work was subsidized with Special Funds for the Major State Basic Research Projects G1990650 and the Chinese National Science Fund No. 20173033.

ИЗВОД

ПРОУЧАВАЊЕ СТАБИЛНОСТИ САМОФОРМИРАНОГ МОНОСЛОЈА
N-ВИНИЛКАРБАЗОЛА ПРИ ЗАШТИТИ БАКРА ОД КОРОЗИЈЕCHUN-TAO WANG,¹ SHEN-HAO CHEN,^{1,2} HOU-YI MA,¹ LAN HUA¹ и NAI-XING WANG¹

¹Department of Chemistry, Shandong University, Jinan 250100, P. R. China, u
²State Key Laboratory for Corrosion and Protection, Shenyang 110015, P. R. China

Образовани су монослојеви N-винилкарбазола на површини бакра процесом самоформирања. Електрохемијске особине површине бакра модификоване монослојем NVC проучаване су методама електродне поларизације и електрохемијском импедансном спектроскопијом (EIS). Поларизациона мерења су показала да присуство монослоја NVC утиче на смањење анодне и катодне реакције на бакарним електродама у раствору 0,5 mol dm⁻³ растворима. Резултати добијени методом EIS показују да се формира густо паковани филм који је у стању да инхибира корозионе процесе. Рендгенска фотоелектронска спектроскопија (XPS) узорака бакра и атомска апсорпциона анализа раствора показале су да је површина бакра превучена самоформираним монослојем NVC, као и да је адсорпција NVC на бакру праћена растварањем Cu у раствор.

(Примљено 17. јануара, ревидирано 28. јуна 2002)

REFERENCES

1. A. Ulman, *Chem. Rev.* **96** (1996) 1533
2. J. D. Swalen, D. L. Allara, D. L. Allara, J. D. Andrade, E. A. Chandross, S. Garoff, J. Israelachvili, T. J. McIlrath, R. Murray, R. F. Pease, J. F. Rabolt, K. J. Wynne, H. Yu, *Langmuir* **3** (1987) 932
3. G. K. Jennings, P. E. Laidinis, *Colloids Surf. A* **116** (1996) 105
4. P. E. Laibins, G. M. Whitesides, *J. Am. Chem. Soc.* **114** (1992) 9022
5. Y. Q. Feng, W. K. Teo, K. S. Siow, Z. Q. Gao, K. L. Tan, A. K. Hsieh, *J. Electrochem. Soc.* **144** (1997) 55
6. Y. Yamamoto, H. Nishihara, K. Aramaki, *J. Electrochem. Soc.* **140** (1993) 436
7. Z. Quan, X. Wu, S. Chen, S. Zhao, H. Ma, *Corros.* **57** (2001) 195
8. Z. Quan, S. Chen, X. Cui, Y. Li, *Corros.* **58** (2002) 248
9. V. D. Castro, F. Allegretti, C. Baldacchini, M. G. Betti, G. Contini, V. Corradini, F. Lamactar, C. Mariani, *Surface Science* **507-510** (2002) 7
10. H. P. Lee, K. Nobe, *J. Electrochem. Soc.* **133** (1986) 2035
11. C. Deslouis, B. Tribollet, G. Menagoli, M. M. Musiani, *J. Appl. Electrochem.* **18** (1988) 374
12. O. E. Barcia, O. R. Mattos, N. Pebere, B. Tribollet, *J. Electrochem. Soc.* **140** (1993) 2825
13. Y. Feng, W.-K. Teo, K.-S. Siow, K.-L. Tan, A.-K. Hsieh, *Corros. Sci.* **38** (1996) 369

14. K. Tokuda, T. Gueshi, H. Matsuda, *J. Electroanal. Chem.* **102** (1979) 41
15. E. Sabatani, I. Rubinstain, R. Maoz, J. Sagiv, *J. Electroanal. Chem.* **219** (1987) 365
16. M. E. Folger, S. B. Ribotta, S. G. Real, L. M. Gasse, *Corros.* **58** (2002) 240
17. H. Ma, S. Chen, L. Niu, S. Zhao, S. Li, D. Li, *J. Appl. Electrochem.* **32** (2002) 65
18. J. B. Brzoska, N. Shahidzadeh, F. Rondelez, *Nature* **360** (1992) 719
19. C. Schonenberger, J. A. M. Sondag-Huathorst, J. Jorritsma, L. G. J. Fokkink, *Langmuir* **10** (1994) 611.